

A SYSTEM FOR REALISTIC WEATHER RENDERING

Kirk Riley
Purdue University
kriley@ecn.purdue.edu

David Ebert *
Purdue University
ebertd@purdue.edu

Charles Hansen
University of Utah
hansen@cs.utah.edu

Jason Levit
University of Oklahoma
jlevit@ou.edu

Abstract—Weather visualization has traditionally been restricted to surface models and 2-D representations. We present a visually accurate method for rendering volumetric multi-field weather data that includes cloud water, ice, rain, snow, and graupel hydrometeors. This representation better communicates the complex 3-D nature of weather, by rendering it according to physically based lighting and scattering characteristics of hydrometeor particles. The rendering system works with the new Weather Research and Forecasting (WRF) NWP model as well as cumulus cloud dynamics models. We have successfully rendered a simulated WRF supercell storm at interactive rates with high visual accuracy. Therefore, improved NWP model evaluation can be achieved through this new visually accurate system. This software has potential uses in, not only weather forecasting and research, but in the education of weather spotters and the general public.

1 INTRODUCTION

Weather visualization is currently dominated by two-dimensional slicing techniques. While this is extremely useful for conveying particular numerical results of synoptic scale phenomena, it is ill-suited for conveying structures of mesoscale and microscale storm phenomena. Although 3-D isosurface techniques have enjoyed some use in the analysis of storms, they do not resolve the complex 3-D nature of evolving storms. The interaction of multiple opaque plastic surfaces, like that shown in Figure 1 is very different from the interaction of translucent multiple particle field densities scattering light.

Weather spotting is a useful technique for understanding and predicting severe storms. Therefore the representation of fields in a realistic fashion provides insight to the complex 3-D phenomenon that is an evolving storm. For example, by presenting the cloud field as "puffy" and the ice anvil as "wispy" with appropriate opacities, the structure of the storm is presented as it would naturally appear, and thus would be informative to anyone trained to observe storms. It provides an answer to "What would my data look like in the sky?". For illustration purposes, such as training applications, the system contains an option for the addition of simulated turbulent detail to create more compelling images.

There are many applications for an accurate weather visualization system. Images similar to observed weather phenomena can enhance prediction. Visually accurate representations can improve the understanding of the optical properties of clouds, and educational applications can create more meaningful severe storm images from simulations with our system.

In Section 2 we will summarize previous work in weather visualization and rendering. In Section 3 we discuss the weather model input into the system. We provide an overview

* Corresponding author address:
MSEE 274
Purdue University
West Lafayette, IN 04907

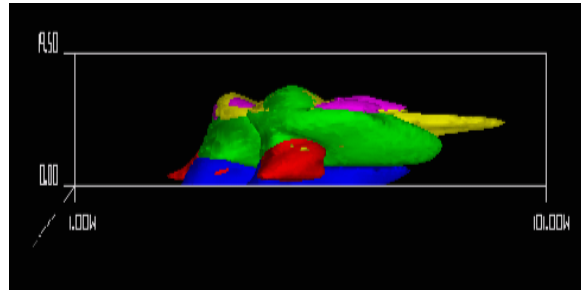


Fig. 1. Isosurface Rendering of Storm Scale Data

of the system capabilities in Section 4. In Section 5 we give an overview of the rendering methodology applied to this data. Section 6 presents some results produced by this system followed by future research directions in Section 7, and conclusions in Section 8.

2 PREVIOUS WORK

The problem of visualizing weather has been examined extensively (Papathomas *et al.*, 1988), (McCaslin *et al.*, 2000), (Trembilski, 2002), (Kniss *et al.*, 2002). Vis5d (Hibbard & Sante, 1986) is a popular tool for multi-variable visualization of weather. IBM (Treinish, 1997) and Georgia Tech (Tian-yue *et al.*, 2001) have done significant work in weather visualization. While these are all very useful tools, they do not create a visually accurate representation.

The rendering of atmospheric phenomena is an active area in graphics research, from early works in (Blinn, 1982) and (Kajiya & Von Herzen, 1984) to more modern techniques in (Max, 1995), (Klassen, 1987), (Nishita *et al.*, 1996), (Preetham *et al.*, 1999), (Dobashi *et al.*, 2002), (Harris & Lastra, 2001), (Stam, 1995). These systems have described the rendering of atmospheric bodies, but do not handle the need for multi-field, accurate renderings at interactive frame rates.

Volume rendering is also an important area in graphics research. From early work in (Drebin *et al.*, 1988) to more recent extensions in gaseous and hardware accelerated rendering in (Ebert & Parent, 1990), (Engel *et al.*, 2001), (Kniss *et al.*, 2003), (Jensen & Christensen, 1998)

The use of simulated detail has seen extensive use in computer graphics. (Perlin & Hoffert, 1989) provides a useful framework for the addition of simulated detail. (Stam & Fiume, 1995) uses warped blobs, and (Ebert *et al.*, 2003) cover many different systems for adding simulated detail.

Variable	Definition
$LWC_{\text{field}}(\vec{s})$	Liquid Water Content of the given field at \vec{s}
ρ_{air}	Density of air $\frac{\text{kg}}{\text{m}^3}$
ρ_{field}	Density of individual particles in field $\frac{\text{kg}}{\text{m}^3}$
$V_{\text{particle}}^{\text{field}}$	Volume of a single particle of the given field m^3
η^{field}	Particle concentration, $\frac{\text{particles}_{\text{field}}}{\text{volume}}$
$T(\vec{s}, \vec{l})$	Light attenuation between points \vec{s} and \vec{l}
$L_l(\vec{s}, \Omega)$	Light contribution at point \vec{s} in Ω direction
β_{ex}	Extinction coefficient $\frac{1}{\text{m}}$
$\beta_{\text{ex}}^{\text{field}}$	Extinction coefficient for given field $\frac{1}{\text{m}}$
$\sigma_{\text{ex}}^{\text{field}}$	Extinction cross-section for given field $\frac{1}{\text{m}^2}$
$P(\Omega, \vec{s})$	Scattering phase function at \vec{s}
ω_{field}	Single scattering albedo of the given field

TABLE I
VARIABLES LIST

Hydrometeor	Equivalent Radius (mm)
Cloud	0.01
Ice	1
Rain	1
Snow	2
Graupel	2.5

TABLE II
EQUIVALENT SPHERICAL PARTICLE CROSS SECTIONS

3 WEATHER DATA

The system is designed to translate the mass ratio liquid water content at a given point in space, $LWC_{\text{field}} = \frac{kg_{\text{field}}}{kg_{\text{air}}}$, into the optical properties of that region. As a reference, Table I lists the variables in this paper. Currently, the system has been applied to the analysis of two different data sets. The first, the Weather Research in Forecasting (WRF) model, contains volumetric cells with the liquid water content for five hydrometeor variables, and many other quantities. Currently we only consider the hydrometeor fields, but future extensions will explore the usage of other weather simulation parameters. These fields include cloud water, rain water, ice, snow, and graupel. For this data set, each volume element is 1 km wide. The second is a model of a smaller cumulus cloud which would be capable of light precipitation that is approximately 6500 meters tall and 6500 meters wide, with 50 m wide volume elements. It was created with a large-eddy simulation from the Straka Atmospheric Model (Straka & Anderson, 1993), as modified in (Carpenter *et al.*, 1998), and initialized with the parameters described in (Lasher Trapp *et al.*, 2001). This model contains only cloud field information, but has much finer details. All particles are assumed to have an equivalent spherical radius, R_{field} . The equivalent particle radii used in this system are given in Table II. The distribution of fields for the multi-field WRF storm, a rendering with per field colors is shown in Figure 2 with the color mapping given in Table III.

Hydrometeor	Color
Cloud	Red
Ice	Magenta
Rain	Blue
Snow	Yellow
Graupel	Green

TABLE III
FIELD COLORS

4 CAPABILITIES OVERVIEW

The program translates a 3-D grid of hydrometeor liquid water contents into an accurately rendered image. This rendering is done at interactive and near interactive rates (between 1-5 frames per second) to allow the user to dynamically explore the data set. Interactive adjustment of scalings on each of the hydrometeor values is possible. The light may be adjusted interactively as well. Because the lighting model makes the clouds translucent, light adjustment allows the user to gain more insight into the inner structure of the cloud. The lighting parameters, such as the albedo of the particles and the angle used for the small angle translucency approximation are also adjustable. For more training oriented applications, additional simulated detail may be added to enhance the visual experience. The parameters for this turbulence are also interactively adjustable for each field, allowing different levels of detail for the various fields.

5 SYSTEM METHODOLOGY

In order to render accurately the multiple particle field densities, we first translate the liquid water content (in $\frac{kg_{\text{field}}}{kg_{\text{air}}}$) of the various fields into particle densities, and scattering coefficients as described in Section 5.1. The particles interact with light differently, and thus we utilize the multiple particle field scattering function described in Section 5.2. We use volume rendering with a volumetric light transport approximation to translate these optical properties into an image as described in Section 5.3.

5.1 Extinction and Scattering

We first need to determine how much light is attenuated as it traverses the samples of the volume. This transparency is an exponential function of the optical depth of the material. Extinction of light is caused by the absorption and outscattering

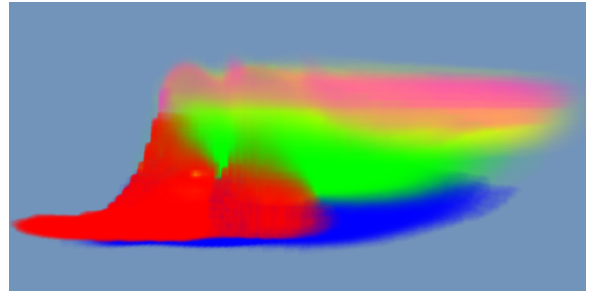


Fig. 2. Cloud with Colored Hydrometeor Fields

of light by particles along a path. In this section we discuss how we apply the LWC and equivalent spherical radii, R_{field} of the particles to calculate the rates of extinction and scattering. Absorption is the light absorbed by particles and not re-emitted. Scattering is the portion of the light lost along the path that is simply redirected through interaction with the particle. The ratio of the scattered light to the total extinction is the particle albedo. Additionally, because hydrometeor particles are high-albedo and relatively large with respect to the wavelength of light, they have scattering cross-sections approximately equal to twice their geometric cross sections.

$$\sigma_{ex}^{field} \approx 2\pi R_{field}^2 \quad (1)$$

The concentration of the particles in a region of space is also necessary to calculate the extinction and scattering. To obtain this value, we require the density of the particle, and the density of air in that region of space (ρ_{field} and $\rho_{air}(\vec{s})$). The particle concentration, for the given field ($\eta_{field}(\vec{s})$) is given in Equation 2.

$$\eta_{field}(\vec{s}) = \frac{\rho_{air}(\vec{s})LWC_{field}(\vec{s})}{\rho_{field}V_{particle}^{field}} \quad (2)$$

The extinction per unit length at \vec{s} , $\beta_{ex}(\vec{s})$, is the probability per unit length of striking a particle, which is given in Equation 3 for the non-overlapping particle approximation.

$$\beta_{ex}^{field}(\vec{s}) \approx \sigma_{ex}^{field} \eta_{field}(\vec{s}) \quad (3)$$

For an equivalent particle radius, we approximate the $\beta_{ex}^{field}(\vec{s})$ with Equation 4.

$$\beta_{ex}^{field}(\vec{s}) \approx \frac{3\rho_{air}(\vec{s})LWC_{field}(\vec{s})}{2\rho_{field}R_{field}} \quad (4)$$

As described, the albedo, ω_{field} is the ratio of scattering to extinction.

$$\omega_{field} = \frac{\beta_{sca}^{field}}{\beta_{ex}^{field}} \quad (5)$$

Thus if we assume near unity albedo, $\beta_{sca}^{field} \approx \beta_{ex}^{field}$. The overall scattering coefficient at a given region of space is given in Equation 6.

$$\beta_{ex}(\vec{s}) = \sum_{All\ Fields} \beta_{ex}^{field}(\vec{s}) \quad (6)$$

To calculate the transparency of a sample between \vec{s} and \vec{w} , we integrate $\beta_{ex}(\vec{s})$ over the sample.

$$T(\vec{s}, \vec{w}) = e^{-\int_{\vec{s}}^{\vec{w}} \beta_{ex}(\vec{s}) ds} \quad (7)$$

This is the multiplicative factor that determines how much light intensity traverses the sample. This is the transparency for a volumetric region of multiple interacting particle densities. To illustrate the difference, compare the image in Figure 4 with Figure 3. The former has per field extinction, whereas the latter has only a single field. Note that the cirrus layer is thinner, while the cloud layer is noticeably more opaque.

5.2 Per Field Particle Scattering

When light intersects scatters from a particle, the resulting probability density function of its exit direction, given the input direction, is the particle scattering, or phase function.

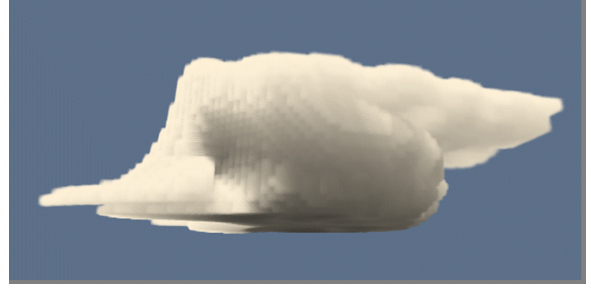


Fig. 3. Incorrect Extinction



Fig. 4. Correct Extinction

To calculate the phase function for multiple particles in space we weigh the scattering phase functions of each of the fields by the total contribution of that field to the scattering coefficient at that point in space. Water and ice scatter light very differently. Ice, due to its hexagonal nature, is more likely to scatter light at angles normal to the incident angle, whereas water will have stronger forward scattering. We use normalized values from those calculated in (Wendling *et al.*, 1979) as shown in Figure 5. Due to limited data, this model has the same phase

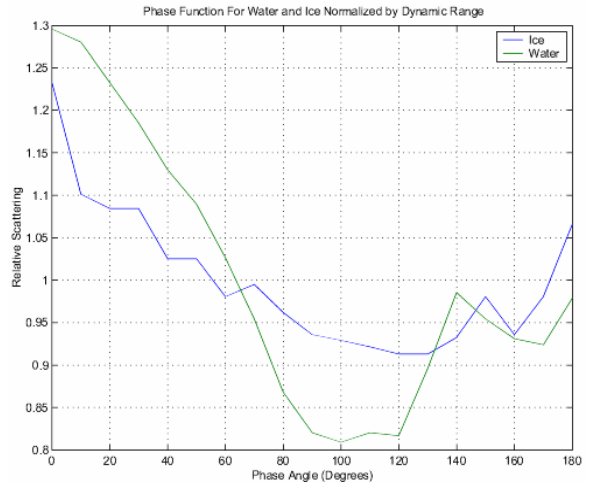


Fig. 5. Normalized Phase Functions for Ice and Water

applied to water and rain, while the ice, snow, and graupel had

another.

$$P(\Theta, \vec{s}) = \frac{\sum_{\text{AllFields}} P_{\text{field}}(\Theta) \beta_{\text{sca}}^{\text{field}}(\vec{s})}{\sum_{\text{AllFields}} \beta_{\text{sca}}^{\text{field}}(\vec{s})} \quad (8)$$

For comparative purposes, an image with equal phase functions per field, and one with a different phase per field are shown in Figure 6.



Fig. 6. Illumination with (a) Same Phase for All Particles and (b) Particle Specific Phase

5.3 Rendering

Now that we have the transparency of the samples, we can volume render the result. The equation we implement is given in Equation 9.

$$L(\vec{w}) = T(0, \vec{w})L_{\text{bg}} + \int_0^{\vec{w}} T(\vec{s}, \vec{w}) \beta_{\text{sca}}(\vec{s}) \int_{4\pi} P(\psi(\Omega)) L_1(\vec{s}, \Omega) d\Omega d\vec{s} \quad (9)$$

This essentially says that the light reaching the eye at \vec{w} is the combination of background light traversing the volume, and the light scattered into the ray between \vec{s} and \vec{w} that survives the volume. The rendering system creates a series of sampling planes, or slices, through the volume, calculates the color on each slice based on the particle concentrations, and blends them together based on the calculated transparency. Depending on the user's desired tradeoff between speed and quality, the number of sampling slices through the volume may be adjusted.

To fully calculate the volumetric light transport is not feasible for interactive light adjustment. Therefore we use a translucency approximation that takes advantage of the forward scattering dominance of hydrometeor particles. The implementation utilizes two rendering buffers: one for the output eye image, and one to store the lighting of the volume. The eye buffer stores $L(\vec{w})$ and the light buffer stores $L_1(\vec{s}, \Omega)$. Because 90% of the light is scattered within ± 10 degrees, we consider light that is scattered within a small angle about the forward direction as forward propagating. We implement the half-angle slicing system and use a translucency calculation similar to (Kniss *et al.*, 2003), with transport parameters set according to the physical properties of clouds. To simplify light transport, the lighting calculation is based on a single phase function. The integral of Cornette and Shanks (Cornette & Shanks, 1992) phase function is used to adjust how much light survives traversal through the volume. This is in contrast to the low-albedo approximation which considers all light that strikes a particle as extinct. A comparison of translucent lighting and low-albedo approximation is given in Figure 7 and Figure 8 respectively. Users interested in more details about the rendering are encouraged to read (Riley *et al.*, 2003) and (Kniss *et al.*, 2003).



Fig. 7. Cloud with Translucent Illumination

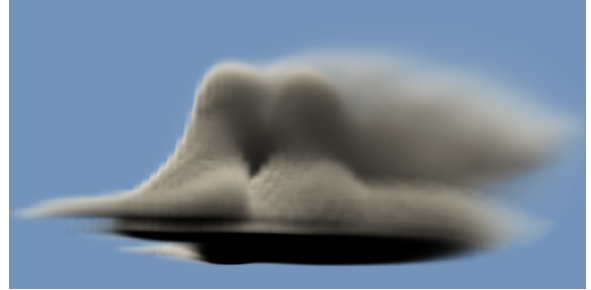


Fig. 8. Low-Albedo Particle Illumination

5.4 Simulated Turbulent Detail

In some applications it is desirable to add detail to existing images in order to produce a more compelling visual experience. To provide this capability we allow the user to specify an amount of additional detail added to the data in order to make the images more realistic. By multiplying the underlying data with a more turbulent noise function, more detail is perceived. For training and educational purposes, this can create images more like what would be expected in the field. Interactive adjustment of the amount of additional detail allows the user great flexibility in creating these images. Images of the WRF storm, with additional detail are shown in Figure 9, Figure 10, Figure 11, and Figure 15. Additionally the cumulus images in Figure 14 utilize simulated detail.



Fig. 9. Large Scale Model with Additional Detail



Fig. 10. Large Scale Model with Additional Detail



Fig. 11. Bottom View of Large Scale Model with Additional Detail

6 RESULTS

For interactive visualization, it must be possible for the user to adjust the relative mixing ratios of the various fields at receive immediate feedback. This system has been applied both to storm scale simulations, Figures 9, 10, 11, 15, and to smaller cloud scale simulations, Figures 14, 12, 13 . For the larger storm simulation, through visually accurate visualization we determined that turbulence, that should have been present, was missing because of the unrealistic smoothness of the cloud.

Modern graphics hardware allows us to adjust the individual field properties without costly recalculation on the data set. In particular, modern pixel shaders allow very flexible adjustment of rendering. The system presented here was implemented on an nVidia GeForceFX 5800 Ultra, using their Cg (C for graphics) compiler for vertex and fragment programs. This system is flexible, but advanced rendering modes come at a price in performance. A table of the frame rates is given in Table IV for a 300×300 image with 128 sampling planes (1 per sample). Simpler modes maintain interactive rates, and the flexibility of programmable hardware allows the user to easily switch to more advanced modes once the coarser parameters have been adjusted and utilize more advanced options.



Fig. 12. Upward View of Cloud Mode, Without Simulated Detail



Fig. 13. Side View of Cloud Model, Without Simulated Detail

7 FUTURE WORK

Now that a framework has been established for rendering particles based on their optical properties, great gains can be achieved by improving the accuracy of those properties. By implementing better characterizations of the particle sizes and improved particle scattering data, the system will produce more accurate images. Extending the system to interact with extra variables in the simulation will also increase its usability. Improving the light transport approximation will also make more realistic representations of the data. Additionally, allowing the cloud models to interact with the sky produces spatial visual cues and improve sense of scale. Improved map projections



Fig. 14. Time Series of a Cloud Scale Visualization With Simulated Detail



Fig. 15. Time Series of the Supercell Storm With Simulated Detail

allow application of the system to a wider range of user data.

8 CONCLUSIONS

We have developed a new visually accurate multi-field weather visualization system that effectively conveys finely varying atmospheric data detail, improves the assessment of weather models, aids the training of weather observers, and presents more complete information in an intuitive style. Volumetric rendering systems are useful for weather data because of their capability to show varying degrees of opacity in inhomogeneous cloud systems. Translucent lighting based on the forward dominance of cloud particles allows the user to simultaneously gain insight to inner structures, while observing the overall structure of the cloud. Our rendering system utilizes the individual extinction and scattering of these atmospheric particles to produce a realistic representation that also provides insight into the structure of the cloud. Already, this system has been useful in determining missing turbulence components in one of the simulated models. To increase the realism of images, simulated turbulent detail may be added to improve the

appearance of the fields based on their properties. The usage of modern hardware maintains interactive rates for simpler modes of the system, and the ability to quickly change modes in the system.

ACKNOWLEDGEMENT

The authors wish to thank Professor Sonia Lasher-Trapp for her aid with the micro-scale cloud data set. Special thanks to Dr. Jerry Tessendorf for his many insightful suggestions. The authors appreciate Nikolai Svakhine's volume renderer contribution. We would also like to thank Martin Kraus for his feedback and the reviewers for their suggestions and helpful comments. This work has been supported by the US National Science Foundation under grants: NSF ACI-0222675, NSF ACI-0081581, NSF ACI-0121288, NSF IIS-0098443, NSF ACI-9978032, NSF MRI-9977218, NSF ACR-9978099 and the US Department of Energy's VIEWS program.

REFERENCES

- Blinn, J.F. 1982. Light Reflection Functions for Simulation of Clouds and Dusty Surfaces. *Computer Graphics*, **8**(3), 21–28.
- Carpenter, R. L. Jr., Droegemeier, K. K., & Blyth, A. M. 1998. Entrainment and detrainment in numerically simulated cumulus congestus clouds. Part I: General results. *J. Atmos. Sci.*, **55**, 3417–3432.
- Cornette, William M., & Shanks, Joseph G. 1992. Physically Reasonable Analytic Expression for the Single-Scattering Phase Function. *Applied Optics*, **32**(16), 3152–3160.

Mode	Frame Rate
Uniform Phase Low-Albedo Light	5.1 fps
Uniform Phase Translucent Light	4.3 fps
Per Field Phase, Translucent Light	1.7 fps
Per Field Phase, Simulated Detail, Translucent Light	1.2 fps

TABLE IV

RENDERING SPEEDS (IN FRAMES/SECOND) FOR VARIOUS MODES

- Dobashi, Yoshinori, Yamamoto, Tsuyoshi, & Nishita, Tomoyuki. 2002. Interactive Rendering of Atmospheric Scattering Effects Using Graphics Hardware. *Proc. Graphics Hardware*, 99–108.
- Drebin, R.A., Carpenter, L., & Hanrahan, P. 1988. Volume Rendering. *Computer Graphics (SIGGRAPH '88 Proc.)*, 22(Aug.), 65–74.
- Ebert, David, Musgrave, Kenton, Peachey, Darwyn, Perlin, Ken, & Worley, Steven. 2003. *Texturing and Modeling A Procedural Approach*. 3 edn. Morgan Kaufman Publishers.
- Ebert, David S., & Parent, Richard E. 1990. Rendering and Animation of Gaseous Phenomena by Combining Fast Volume and Scanline A-buffer Techniques. *Computer Graphics*, 24(4), 357–366.
- Engel, Klaus, Kraus, Martin, & Ertl, Thomas. 2001. High-Quality Pre-Integrated Volume Rendering Using Hardware-Accelerated Pixel Shading. *Proceedings of the ACM Siggraph/Eurographics Workshop on Graphics Hardware 2001*, 9–16.
- Harris, M. J., & Lastra, A. 2001. Real-Time Cloud Rendering. *Eurographics 2001 Proceedings*, 20(3), 76–84.
- Hibbard, W., & Sante, D. 1986. 4-d Display of Meteorological Data. *Proceedings of 1986 Workshop on Interactive 3D Graphics*, 129–134.
- Jensen, H.W., & Christensen, P.H. 1998. Efficient Simulation of Light Transport in Scenes with Participating Media Using Photon Maps. *Proceedings SIGGRAPH '98, Computer Graphics Proc, Ann Conf. Series*, 311–320.
- Kajiya, James T., & Von Herzen, Brian P. 1984. Ray Tracing Volume Densities. *Computer Graphics*, 18(3), 165–174.
- Klassen, Victor R. 1987. Modeling the Effect of the Atmosphere on Light. *ACM Transactions on Graphics*, 6(3), 215–237.
- Kniss, Joe, Hansen, Charles, Grenier, Michel, & Robinson, Tom. 2002. Volume Rendering Multivariate Data to Visualize Meteorological Simulations: A Case Study. *IEEE Visualization Symposium*, 189–194.
- Kniss, Joe, Premoze, Simon, Hansen, Charles, Shirley, Peter, & McPherson, Allen. 2003. A Model for Volume Lighting and Modeling. *IEEE Transactions on Visualization and Computer Graphics 2003*, 9(2), 109–116.
- Lasher Trapp, S.G., Knight, C.A., & Straka, J.M. 2001. Echoes from Ultrajiant Aerosol in a Cumulus Congestus: Modeling and Observations. *J. Atmos. Sci.*, 58, 3545–3562.
- Max, Nelson. 1995. Optical Models for Direct Volume Rendering. *IEEE Transactions on Visualization and Computer Graphics*, 1(2), 99–108.
- McCaslin, P. T., McDonald, P. A., & Szoke, E. J. 2000. 3D Visualization Development at NOAA Forecast Systems Laboratory. *Computer Graphics*, 34(1), 41–44.
- Nishita, Tomoyuki, Dobashi, Yoshinori, & Nakamae, Eihachiro. 1996. Display of Clouds Taking into Account Multiple Anisotropic Scattering and Sky Light. *Proceedings of the 23rd Annual Conference on Computer Graphics and Interactive Techniques*, 379–386.
- Papathomas, T.V., Schiavone, J.A., & Julesz, B. 1988. Applications Of Computer Graphics To The Visualization Of Meteorological Phenomena. *Computer Graphics*, 22(4), 327–334.
- Perlin, Ken, & Hoffert, Eric. 1989. Hypertexture. *Computer Graphics*, 23(3), 253–262.
- Preetham, A. J., Shirley, Peter, & Smits., Brian E. 1999. A Practical Analytic Model for Daylight. *Pages 91–100 of: Rockwood, Alyn (ed), Siggraph 1999, Computer Graphics Proceedings*. Los Angeles: Addison Wesley Longman, for ACM Siggraph.
- Riley, K., Ebert, D., Hansen, C., & Levit, J. 2003. Visually Accurate Multi-Field Weather Visualization. *Proceedings of IEEE Visualization 2003*, 279–286.
- Stam, Jos. 1995. Multiple Scattering as a Diffusion Process. *Proceedings of the 6th Eurographics Workshop on Rendering, Dublin, Ireland, June*, 51–58.
- Stam, Jos, & Fiume, Eugene. 1995. Depiction of Fire and Other Gaseous Phenomena Using Diffusion Processes. *SIGGRAPH 95 Conference Proceedings, Annual Conference Series*, Aug., 129–136.
- Straka, J. M., & Anderson, J. R. 1993. Numerical simulations of microburst-producing storms: Some results from storms observed during COHMEX. *J. Atmos. Sci.*, 50, 1329–1348.
- Tian-yue, Jiang, Ribarsky, William, Wasilewski, Tony, Faust, Nickolas, Hannigan, Brendan, & Parry, Mitchell. 2001. Acquisition and Display of Real-time Atmospheric Data on Terrain. *Eurographics-IEEE Visualization Symposium 2001*, 15–24.
- Treinisch, Lloyd A. 1997. Regional Weather Forecasting in the 1996 Summer Olympic Games Using an IBM SP2. *Proceedings of the AMS 13th IIPS*, Feb.
- Trembilski, Andrzej. 2002. Transparency for Polygon Based Cloud Rendering. *Proceedings of the 2002 ACM Symposium on Applied Computing*, 785–790.
- Wendling, Peter, Wendling, Renate, & Weickman, Helmut K. 1979. Scattering of Solar Radiation by Hexagonal Ice Crystals. *Applied Optics*, 18(15), 2663–2671.